Article

A Study of Sewage Sludge Co-Combustion with Australian Black Coal and Shiitake Substrate

Guan-Bang Chen [1],*, Samuel Chatelier [2], Hsien-Tsung Lin [3], Fang-Hsien Wu [1] and Ta-Hui Lin [1,2],*

[1] Research Center for Energy Technology and Strategy, National Cheng Kung University, Tainan 70101, Taiwan; z10602031@email.ncku.edu.tw

[2] Department of Mechanical Engineering, National Cheng Kung University, Tainan 70101, Taiwan; n16057164@mail.ncku.edu.tw

[3] Department of Aeronautics and Astronautics, National Cheng Kung University, Tainan 70101, Taiwan; P48021027@mail.ncku.edu.tw

* Correspondence: gbchen@mail.ncku.edu.tw (G.-B.C.); thlin@mail.ncku.edu.tw (T.-H.L.); Tel.: +886-6-275-7575 (ext. 51030) (G.-B.C.); +886-6-2757575 (ext. 51031) (T.-H.L.)

check for updates

Abstract: Co-combustion technology can be a gateway to sewage sludge valorization and net CO_2 reduction. In this study, combustion characteristics of sewage sludge, Australian black coal, shiitake substrate, and their blends were analyzed via thermogravimetric analysis (TGA) coupled with Fourier transform infrared spectroscopy. The ignition temperature, burnout temperature, flammability index (*C*), and combustion characteristics index (*S*) of the fuels and their respective blends were estimated. Kinetic parameters were also estimated using the Coats-Redfern method. The results showed that the oxidation of the blends had two distinct stages. Synergistic effects existed for all the blends, with negative ones occurring at temperatures between 300 and 500 °C and positive ones during the char oxidation period. In the first oxidation stage, both *C* and *S* indexes increased with sludge addition to the coal. However, they decreased with sludge addition in the final oxidation stage. The catalytic effect of the sludge and the shiitake was pronounced in the final oxidation stage and it resulted in a decrease of activation energy. As for the pollutant emissions, the results showed that NO_x and SO_2 emissions decreased for 25 wt.% sludge addition to the coal. For the sludge-shiitake blends, NO_x and SO_2 emissions decreased with increasing shiitake addition. The single-pellet combustion results showed that ignition delay time reduced with increasing sludge/coal ratio but increased with increasing sludge/shiitake ratio. The volatile combustion duration decreased with the addition of sludge and total combustion time decreased sharply with increasing sludge ratio.

Keywords: co-combustion; sewage sludge; thermogravimetric analysis; Fourier transform infrared spectroscopy; synergistic effect; single-pellet combustion

1. Introduction

Sewage sludge is a common by-product resulting from the treatment processes of industrial or municipal wastewaters. Its global production has increased considerably in the past years. This increase is expected to continue in the coming years as more and more people move to urban areas. In 2012, around 2.37 million tons of sludge were produced in Taiwan [1]. If not properly disposed of, sewage sludge can be a threat to the environment and human health because of the high presence of heavy metals and pathogens [2,3].

Prior to disposal, sewage sludge is usually processed in order to reduce smell, the quantity of organic solids, water content, and to eliminate some disease-causing bacteria. Therefore, at the wastewater

treatment plant, the sludge goes through different processes such stabilization, conditioning and dewatering [4]. Traditionally, sewage sludge is disposed of through landfilling at sanitary sites and agricultural use (directly or indirectly). Currently, most of the sludge produced in Taiwan is disposed of through landfilling [1]. In the future, with the scarcity of available land, stricter environmental regulations, rising concerns regarding health and safety, and willingness to build and promote a circular economy model, it is expected that these practices will change. Sewage sludge can also be disposed of through incineration or thermally processed to recover its energy content.

Sewage sludge has been classified as biomass [5] due to its high calorific value and as semi-biomass [6] in the literature. It is even sometimes compared to low-rank coals such as lignite in terms of energy content [7,8]. However, sewage sludge differs from plant biomass in many aspects, which might pose technical challenges to its combustion. Describing the combustion process of sewage sludge is not an easy task due to the large heterogeneity in the physical and chemical properties. Cui et al. [9] studied the combustion process of pelletized raw sewage sludge and found that, as with biomass particle, sewage sludge combustion comprises different stages, such as drying, devolatilization, volatiles combustion, and char combustion. Each stage of combustion may last for a specific time depending on the fuel physical and chemical characteristics and some external parameters, such as the combustor configuration, heat and mass transfer with the surroundings, heating rate, and particle size [9,10]. At a relatively low heating rate and for a small particle, there is a clear distinction between the stages. However, at higher heating rates and for larger particles, there is a certain degree of overlap between the stages [11]. High inorganic matter contents in sludge might pose some challenges to its combustion process. Slagging (alkali-induced or silica-melt induced), ash accumulation in the furnace (fouling), corrosion, ash handling, heavy metals and emission levels are potential major issues for sludge combustion.

From a waste minimization viewpoint, sewage sludge incineration has the advantage that sludge with a wider range of water content may be used, and therefore requires less pretreatment. However, for sludge energetic valorization, such a process can be energy-deficient as supplementary fuel might be required to handle the wet sludge. Therefore, co-utilization of sludge with other fuels may be more feasible from an energy perspective. Sludge co-combustion also offers some economic advantages as there is no need to hire new experienced personnel and existing facilities and devices for gaseous emissions control can be used; consequently, no additional investments are needed for a new processing plant [12]. From an environmental viewpoint, co-combustion of sewage sludge and coal can help reduce net CO_2 emissions. Currently, sewage sludge is co-fired with coal in power plants, with other biomass, with municipal solid waste in incinerators, and in clay brick manufacture and cement kilns [13,14].

During co-combustion, dried sewage sludge replaces only a small fraction of the plant's feedstock. Werther and Ogada [4] reported that sludge should be milled and dried, leaving a water content of less than 10%, when co-fired with bituminous coal in pulverized coal power stations. Otero et al. [15] stated that dried sludge can be co-fired at a percentage of up to 50% with no major consequences regarding gaseous emissions. Thermogravimetric analysis (TGA) is widely used in studies on the thermal degradation of sludge co-combustion. Nimoya et al. [16] showed that sludge co-combustion with coal has better performance than sludge mono-combustion. An investigation by Folgueras et al. [17] using TGA of sewage sludge and bituminous coal blends revealed that blends with a sludge content of 10% behave similarly to coal, whereas blends of 50% clearly show two combustion stages (a clear volatile matter and more reactive structures stage and a second thermal decomposition stage of more complex structures).

However, few studies have elaborated on sludge co-combustion with plant biomass. Kijo-Kleczkowska et al. [18] studied the co-combustion of pelletized sewage sludge with coal and biomass, and reported that adding sludge to biomass (willow Salix viminalix) increases the fuel ignition temperatures, whereas increasing the sludge percentage in sludge-coal (lignite) blends decreases the ignition temperature due to the presence of volatiles. It is expected that mixing low-grade

biomass with higher-quality biomass may reduce flame stability problems while minimizing corrosion due to the deposition of ash, which contains low-melting-point salts.

　　　Although there are many studies on sludge co-combustion in the literature, further study is still essential to research the co-combustion behavior and interaction due to the complicated composition of sludge and the diversity of biomass species. Therefore, this study investigates sludge co-combustion with coal and biomass by means of TGA and single-pellet combustion experiments. The selected biomass is a mushroom growing substrate, which is one of the major agricultural wastes in Taiwan. Subsequently, the kinetic parameters and the emission characteristics are also investigated using the Coats-Redfern integral method and Fourier transform infrared spectroscopy (FTIR), respectively. The existence of synergistic effects with addition of sludge to the blends is also taken into account.

2. Materials and Methodology

2.1. Sample Pretreatment

　　　Original sewage sludge was obtained from a WWTP in Tainan City, Taiwan (R.O.C.). In the as-received (ar) basis (Figure 1a), the sludge had a water content of more than 50%. Prior to composition analysis, the sludge was sun-dried to reduce its moisture content; the process is shown in Figure 1b. The final sun-dried sewage sludge is referred to as dried sewage sludge (DSS) and is considered as the as-received sludge in this study.
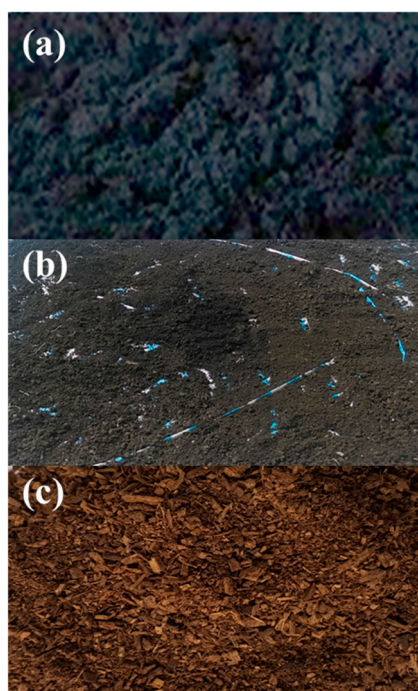

Figure 1. Photographs of different fuels: (**a**) original sewage sludge; (**b**) sun-drying process; (**c**) shiitake growing substrate.

　　　Shiitake mushrooms, originally grown at high altitudes, are now widely grown throughout many areas in Taiwan. They are commonly grown in cultivation bottles or plastic bags, called "space bags" by farmers, filled with mushroom growing substrate (Figure 1c). Sawdust from the lumber industry and most recently chopped dried rice straw chips are used as the mushroom growing substrate [19]. Each year in Taiwan, an estimated 29.6 million bags and 7.5 million bottles are emptied of substrate [20]. The majority is reused to grow other types of mushrooms and eventually become agricultural waste. Shiitake substrate was obtained from a company that recycles agricultural waste. In this study, the term shiitake is used interchangeably with shiitake substrate. As for the coal used in this study (Australian

black coal), it is a sub-bituminous coal and is often used for power generation in Taiwan. It was ground and provided by the Industrial Technology Research Institute.

To ensure homogeneity of the fuels, all the samples were crushed and sieved to a particle size of less than or equal to 96 μm (Mesh #160), and then dried in an oven at 103 °C for 10 h, in order to minimize water content, before composition analysis. To study the co-combustion behavior of sewage sludge mixed with coal and the shiitake substrate, two different blending ratios were defined; a biomass blending ratio (BBR) and a sludge-shiitake ratio (SSR). The two ratios were varied from 0% to 100% in increments of 25%. BBR = 0% represents the case of pure Australian black coal, SSR = 0% represents the case of a pure shiitake substrate, and BBR = SSR = 100% represents the case of pure sewage sludge. To prepare a mixture, a 10 g sample was prepared in a glass cylindrical container and well stirred using spherical steel balls for each case.

2.2. Fuel Properties

The ultimate analysis and proximate analysis of the samples in their as-received (ar) basis was determined through an elemental analyzer (Elementar vario EL III) and a thermal analyzer (PerkinElmer STA 8000), respectively. The proximate was obtained in accordance with the ASTM methods (ASTM D3302-12, ASTM D3175-11, ASTM D3174-11, and ASTM D7582-10e1) [21]. A bomb calorimeter (Parr 6200 Isoperibol Calorimeter) was used according to standardized procedures to estimate the gross calorific value of the samples and their blends. The proximate analysis results and heating values of the oven-dried sewage sludge and shiitake were used to calculate the values on a dry and ash-free (daf) basis.

2.3. Thermogravimetric Analysis

The weight loss history and exothermic phenomenon of the individual fuels and their blends in a linearly heated environment were studied using a thermal analyzer (PerkinElmer STA 8000) which was coupled with a differential scanning calorimetry (DSC) to measure the heat flow into or out of the sample over time. For each experiment, a sample weighing of about 9–10 mg was placed in a small crucible, and then put in a thermal analyzer to study its thermal degradation. The sample was heated from 30 °C to 1000 °C at a heating rate of 20 °C·min^{-1}. Air was used as a carrier gas at a flow rate of 50 mL·min^{-1}. Each experiment was repeated at least twice to ensure reproducibility. The recorded weight loss, namely, the TG curve, of the samples and its first derivative (DTG) were obtained using Pyris Manager software.

2.4. Synergistic Effect Analysis

In order to study whether there existed a coupling synergistic effect [22] between the samples, the calculated weight curves of the mixtures were estimated as the sum of the TGA curves of each individual sample. The calculated weight is denoted as W_{cal}, defined by the linear additive rule expressed by Equations (1) and (2) for the sludge-coal mixture and the blend of sludge and shiitake, respectively.

$$W_{cal} = \left(1 - \gamma_{sludge}\right)W_{coal} + \gamma_{sludge}W_{sludge} \tag{1}$$

$$W_{cal} = \left(1 - \gamma_{sludge}\right)W_{shiitake} + \gamma_{sludge}W_{sludge} \tag{2}$$

where γ_{sludge} represents the weight proportion of sewage sludge in the mixture, and W_{coal}, W_{sludge}, and $W_{shiitake}$ are the TG curves, at 20 °C·min^{-1}, of Australian black coal, sewage sludge, and shiitake, respectively. A positive synergistic effect may exist when the values of the experiment curves, W_{exp}, are lower than that of W_{cal} in the temperature range of the experiment. Equation (3) expresses the deviation between the experimental and the calculated curves, namely, ΔW, from which the degree of

the synergistic effects was evaluated. Sadhukhan et al. [23] used the root mean square (RMS) values of the deviation to measure whether synergistic effects existed.

$$\Delta W = W_{exp} - W_{cal} \tag{3}$$

2.5. Combustion Characteristics Parameters

The intersection method was used in this study to estimate the ignition temperature (T_i) from the TGA results. For further readings regarding this method, one can refer to the studies of Lu et al. [24]. The burnout temperature (T_b) was estimated by the conversion method [24,25], where T_b is defined as the temperature at which the conversion of the fuel reaches 99%.

Knowing both T_i and T_b, two combustion characteristic parameters, namely, the combustion characteristics index (*S*) [25] and the flammability index (*C*) [26], were calculated. Typically, a fuel with a larger value of *S* and *C* has an improved combustion performance and combustion stability, respectively.

2.6. Kinetic Parameters Analysis

Kinetic parameters, obtained using the Coats and Redfern integral method [27], were estimated from the TGA results to further study the combustion characteristics of the samples. The fundamental rate equation of a heterogeneous solid phase reaction can be described by the following equation:

$$\frac{d\alpha}{dt} = k(T)f(\alpha) \tag{4}$$

where α is the conversion degree, expressed as:

$$\alpha = \frac{W_s - W}{W_s - W_e} \tag{5}$$

The temperature dependence of k is expressed by the Arrhenius equation:

$$k(T) = Aexp\left(-\frac{E}{RT}\right) \tag{6}$$

where A is the pre-exponential factor (min^{-1}), E is the apparent activation energy (kJ·mol^{-1}), T is the reaction temperature (K), and R is the gas constant (8.314×10^{-3} $\text{kJ·mol}^{-1}\text{·K}^{-1}$). For non-isothermal and heterogeneous solid phase reactions at a constant heating rate, the temperature increasing rate could be described as $\beta = dT/dt$. Therefore, Equations (4) and (6) can be combined to become:

$$\frac{d\alpha}{dT} = \frac{1}{\beta}\frac{d\alpha}{dt} = \frac{1}{\beta}Aexp\left(-\frac{E}{RT}\right)f(\alpha) \tag{7}$$

The specific form of $f(\alpha)$ represents the hypothetical model of the reaction mechanism or "model function", and can be written as $f(\alpha) = (1 - \alpha)^n$, in the form of an *n*th-order reaction. It is assumed that the conversion function, $f(\alpha)$, depends on the rate of weight loss.

Integration of Equation (7) yields:

For *n* = 1

$$ln\left[\frac{-ln(1-\alpha)}{T^2(1-n)}\right] = ln\left[\frac{AR}{\beta E}\left(1 - \frac{2RT}{E}\right)\right] - \frac{E}{RT} \tag{8}$$

For *n* ≠ 1

$$ln\left[\frac{1 - (1-\alpha)^{1-n}}{T^2(1-n)}\right] = ln\left[\frac{AR}{\beta E}\left(1 - \frac{2RT}{E}\right)\right] - \frac{E}{RT} \tag{9}$$

For the tested temperature ranges and most values of E, $\frac{E}{RT} \geq 1$ and $1 - \frac{2RT}{E} \approx 1$. Thus, Equations (8) and (9) can be further simplified as:

$$ln\left[\frac{-ln(1-\alpha)}{T^2(1-n)}\right] = ln\left(\frac{AR}{\beta E}\right) - \frac{E}{RT}; \; (n=1) \tag{10}$$

$$ln\left[\frac{1-(1-\alpha)^{1-n}}{T^2(1-n)}\right] = ln\left(\frac{AR}{\beta E}\right) - \frac{E}{RT}; \; (n \neq 1) \tag{11}$$

The activation energy (E) and the pre-exponential factor (A) can be obtained from the slope, $-E/R$, and the intercept of the regression line, respectively, by plotting $ln\left[\frac{-ln(1-\alpha)}{T^2(1-n)}\right]$ versus $1/T$ and $ln\left[\frac{1-(1-\alpha)^{1-n}}{T^2(1-n)}\right]$ versus $1/T$. E and A can be used to evaluate the difficulty and intensity of combustion reactions of the fuels, respectively. Different regression lines are plotted for different values of reaction order (n = 0.3, 0.6, 0.9, 1, 1.2, 1.5, 2, and 3). The best fitting ones are used to estimate the activation energy and the pre-exponential factor.

2.7. Fourier Transform Infrared Spectroscopy

Evolved gas products in the TGA experiments were analyzed using a Fourier transform infrared spectrometer (PerkinElmer Spectrum Two FT-IR). To prevent the condensation of less-volatile products, the gas cell and the transfer line were both heated at 280 °C. The FTIR spectra were obtained in the scanning range of 4000 to 600 cm^{-1}, in terms of wavenumber. The resolution and number of accumulations were set to 1 cm^{-1} and 1, respectively. FTIR spectra of the gaseous products were collected continuously. The evolved gas products were obtained and analyzed using the software Spectrum TimeBase. In the study, the studied gases (CH_4, CO, CO_2, NO_x, SO_2) and their wavenumber intervals are listed in Table 1 [28–33]. Finally, the yields of gaseous products are an important indicator to understand the evolved gas from the combustion experiments. Because absorbance varies with species concentration during FTIR quantitative analysis, a normalized value of the gas yield was calculated for better comparison purpose. The gas yield was defined as the ratio of the integral values under the evolution curves of the different gaseous products and the sample initial weight; and is expressed as follow [34]:

$$\text{Gas yield} = \frac{\text{integral value of gaseous product}}{\text{initial sample weight}} \tag{12}$$

Table 1. Wavenumber intervals of different gaseous species.

Gas Species	Wavenumber Range (cm^{-1})	Functional Groups	Ref.
CH_4	3000–2700	C-H	[28]
CO_2	2400–2240	C=O	[29–31]
CO	2240–2060	C-O	[29–31]
NO_x	1795–1520	-NO_2 and -NO	[32,33]
SO_2	1374–1342	S=O	[29,33]

2.8. Single-Pellet Combustion

A dry pressing die set with a diameter of 12.7 mm was used to make the pellets. About 1 g of the sample powder was poured into a steel sleeve and compacted, using a load of about two tons on the pushing rod, with a hydraulic press. This technique was used to make the pure fuels and their respective blended pellets prior to the single-pellet combustion experiments.

Detailed measurement of the behavior of individual pellets of the different fuels might be useful for improving of the modeling and design of a boiler plant. In order to understand the combustion

behavior of different biomass blends and to simulate real furnace conditions, each pellet was burned in a single-pellet free-drop furnace. Figure 2 shows a diagram of the single-pellet combustion system. Two electrically heated plates, controlled by a proportional-integral-derivative controller, provide heat to the furnace and a K-type thermocouple that sends feedback temperature measurements to the controller. Three temperatures (600, 700, and 800 °C) were used in this study. Air was used as the carrier gas for all experiments and the flow was controlled by an electronic flowmeter at 3.5 SLPM. Before entering the combustion chamber, the carrier gas was heated by a preheater. In the experiment, the pellet was dropped through the transmission tube toward the stainless mesh platform, which was connected to a quartz holder. Real-time weight measurements (one data point per second) of the pellet were recorded using an electronic scale with 0.001 g precision. A Sony FDR-AX100 4K camera (30 fps) was used to record video of the pellet combustion process through the observation window. Post-analysis of the video was performed using standard software that allows frame-by-frame viewing.
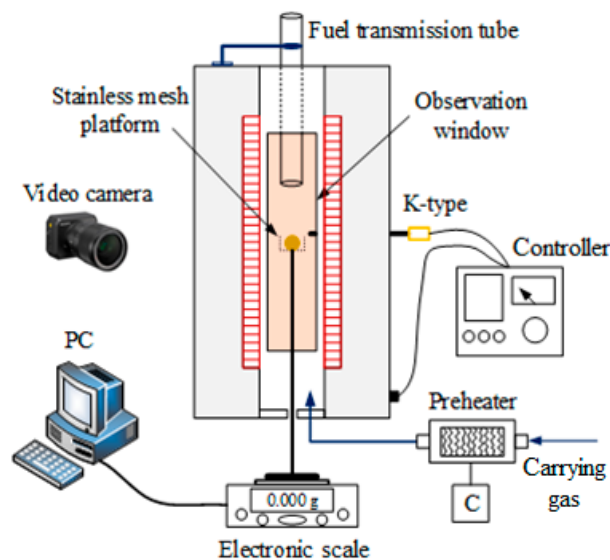

Figure 2. Single-pellet combustion system.

The moment when the scale showed the approximate recorded measurement after the pellet fell on the platform was taken as $t = 0$ s for the weight measurement data. The ignition delay time (t_{id}) was estimated from an analysis of recorded images. t_{id} is the time that it takes for the pellet to ignite after falling into the hot environment. Generally, volatile matter, flammability of volatiles, and transport from the particle determine how ignition of a particle occurs, either homogeneously (gas phase ignition) or heterogeneously. Homogeneous ignition is considered in this study for determining t_{id}. The first frame showing a glowing flame of the burning volatiles is defined as the moment of ignition. According to adiabatic thermal explosion theory, the homogeneous ignition delay time can be estimated as [35]:

$$t_{id} = \frac{c_{v,g}\left(\frac{T_0^2}{T_a}\right)}{q_c Y_{F,0} B exp\left(\frac{-T_a}{T_0}\right)} \tag{13}$$

where $c_{v,g}$ is the specific heat of the background gas (constant volume), T_0 is the initial temperature of the local volatiles and oxidizer mixture, q_c is the heat released by combustion per mass of volatiles, $Y_{F,0}$ is the initial mass fraction of the volatiles and $B exp(-T_a/T_0)$ is the reactivity of the mixture of volatiles and oxidizer. The released volatiles act like a shield, preventing O_2 from diffusing to the sludge particle surface. They ignite and burn in gas phase. After the pellet bursts into flame, the volatiles released are burned homogeneously until extinction. This length of time is demarcated as

the volatile combustion duration t_f in this study. Then, the char keeps burning heterogeneously until the sample weight does not change. Finally, the end of the single-pellet combustion, namely t_{tot} was defined as the time when the measured weight showed no change in a period of 60 s. Each experiment was repeated five times. The average value of the parameters was calculated and reported in this study.

3. Results and Discussion

3.1. Fuel Properties

The ultimate analysis and the proximate analysis results of the samples used in this study are shown in Table 2. The ultimate analysis results of the fuels in their "ar" basis show that sewage sludge was 28.4 wt.% carbon, 5.29 wt.% hydrogen, and 25.58 wt.% oxygen. Compared to Australian coal (73.1 wt.% carbon) and shiitake (40.49 wt.% carbon), sewage sludge has the lowest carbon content. The oxygen content of Australian black coal and shiitake is 5.27 wt.% and 29.03 wt.%, respectively. The results also show that the nitrogen content, 4.65 wt.%, and the sulfur content, 2.66 wt.%, are the highest for sewage sludge. Consequently, the combustion of sludge should receive attention with respect to some pollution and corrosion issues.

Table 2. Ultimate analysis and proximate analysis of sewage sludge, shiitake, and Australian coal.

Sample	Ultimate Analysis (wt.%)				
	C	H	O	N	S
DSS$_{ar}$	28.40	5.29	25.58	4.65	2.66
Shiitake$_{ar}$	40.49	5.95	29.03	3.23	0.38
Australian coal	73.10	4.30	5.27	1.65	0.48

Sample	Proximate Analysis (wt.%)				HHV (MJ·kg^{-1})
	M	VM	ASH	FC *	
DSS$_{ar}$	8.07	48.90	39.61	3.42	11.37
DSS$_{daf}$	-	91.50	-	8.50	21.67
Shiitake$_{ar}$	13.28	69.05	13.52	4.15	15.48
Shiitake$_{daf}$	-	92.83	-	7.17	21.66
Australian coal	1.96	30.77	17.18	50.09	26.10

* Calculated from the difference. ar: as-received basis. daf: dry and ash-free basis.

From the proximate analysis results of the samples, the sun-dried sewage sludge (DSS) was 8.07 wt.% moisture, 48.9 wt.% volatile matter, 39.61 wt.% ash, and 3.42 wt.% fixed carbon. However, drying the sludge and estimating its proximate analysis on an ash-free basis yields 91.5 wt.% and 8.5 wt.% for volatile matter and fixed carbon content, respectively. Shiitake and Australian black coal's volatile matter content on an as-received basis is 69.05 wt.% and 30.77 wt.%, respectively. The fixed carbon content of the shiitake substrate and Australian black coal is 4.15 wt.% and 50.09 wt.%, respectively. The amount of volatiles strongly influences the thermal decomposition and combustion behavior of solid fuels, while the amount of fixed carbon influences the char oxidation process. Australian black coal has the lowest moisture and ash content of the samples; with sewage sludge ash content, 39.61 wt.%, being the highest because of its high inorganic content.

The measured heating value of the individual fuels are also shown in Table 2. Sewage sludge, with a heating value of 11.37 MJ·kg^{-1}, has the lowest HHV of the studied fuels. Such low HHV is perhaps due to the fact that sewage sludge has high inorganic matter and low carbon content. However, taken on an ash-free basis, its HHV increased to 21.67 MJ·kg^{-1}, similar to that of shiitake, 21.66 MJ·kg^{-1}. The HHV of Australian black coal is 26.1 MJ·kg^{-1}. The heating value of the sewage sludge and the shiitake is almost 80% of that of Australian black coal.

3.2. Thermogravimetric Analysis

The combustion profile of sewage sludge is shown in Figure 3. Sludge oxidation occurred in three stages. A dehydration stage, where moisture in the fuel is released, and a combustion stage that can be divided into main and final oxidation stages. The main oxidation stage is referred to as stage 1 in this study, and has a temperature range of 192.60 to 370.78 °C. It might be attributed to the reaction of air with the volatiles and some reactive structures in the sludge. During this stage, the volatiles released did not burn intensely, as shown by the heat flow curve. The maximum oxidation rate in this stage occurs at 286.61 °C. The weight loss during stage 1 is about 24.89 wt.%. The final oxidation stage, stage 2, started at about 370.78 °C, and showed a total weight loss of 25.86 wt.% at 800 °C. It might be attributed to the reaction of air with the heavier components or more complex structures and char oxidation. The maximum oxidation rate occurs at 481.55 °C. Stage 2 is associated with intense heat release, as shown by the DSC curve. Comparing the weight loss rates of the two stages, it is found that the burning rate (-4.80 wt.%·min^{-1}) of stage 1 was faster than that of stage 2 (-3.93 wt.%·min^{-1}), which is due to the high porosity [4] and high surface area [29] of the sludge.
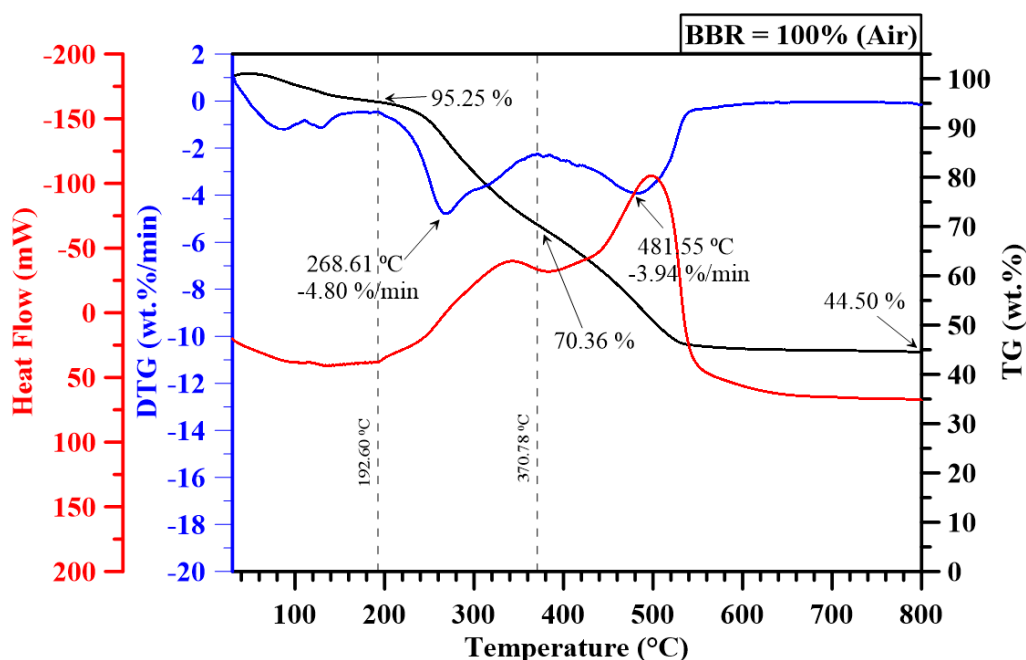

Figure 3. Thermogravimetric analysis results of sewage sludge under combustion condition.

The TGA results of Australian black coal are shown in Figure 4, and display a typical combustion profile of sub-bituminous coal with one-stage thermal decomposition, as shown by the DTG curve. The peak (-6.33 wt.%·min^{-1}) of the burning rate was at 580.73 °C and corresponded to intense heat release, as shown by the DSC curve. This stage is referred to as stage 2 in this study, and it is the result of the devolatilization process as well as char oxidation of the coal. The total weight loss of the oxidation stage at 800 °C is approximately 80.24 wt.%.

Shiitake oxidation occurred in two stages, as shown in Figure 5. Stage 1 showed one peak between 200 and 407 °C with a maximum value of -14.86 wt.%·min^{-1} at 317.54 °C. This peak can be attributed to the release and oxidation of the holocellulose (hemicellulose + cellulose) and a small amount of the lignin in the substrate, showing a total weight loss of about 51.77 wt.%. Further decomposition of the lignin and char oxidation occurred in the final oxidation stage, which showed a burning rate peak, at 439.13 °C, of -6.48 wt.%·min^{-1}. The total weight observed in the final oxidation stages at 800 °C is 27.89 wt.%. At higher temperatures (620–720 °C), a small weight loss can be observed. As this was not associated with any significant heat release, it is not considered as a stage itself and therefore is

included in stage 2. It might be related to an intrinsic characteristic of the substrate, which is beyond the scope of this study.
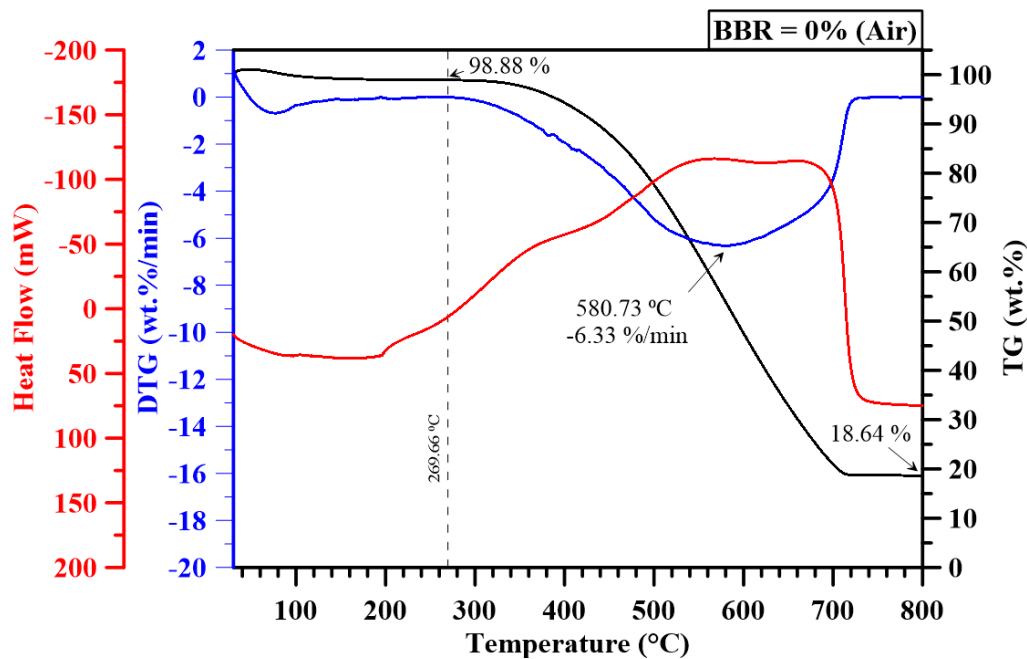

Figure 4. Thermogravimetric analysis results of Australian black coal under combustion condition.
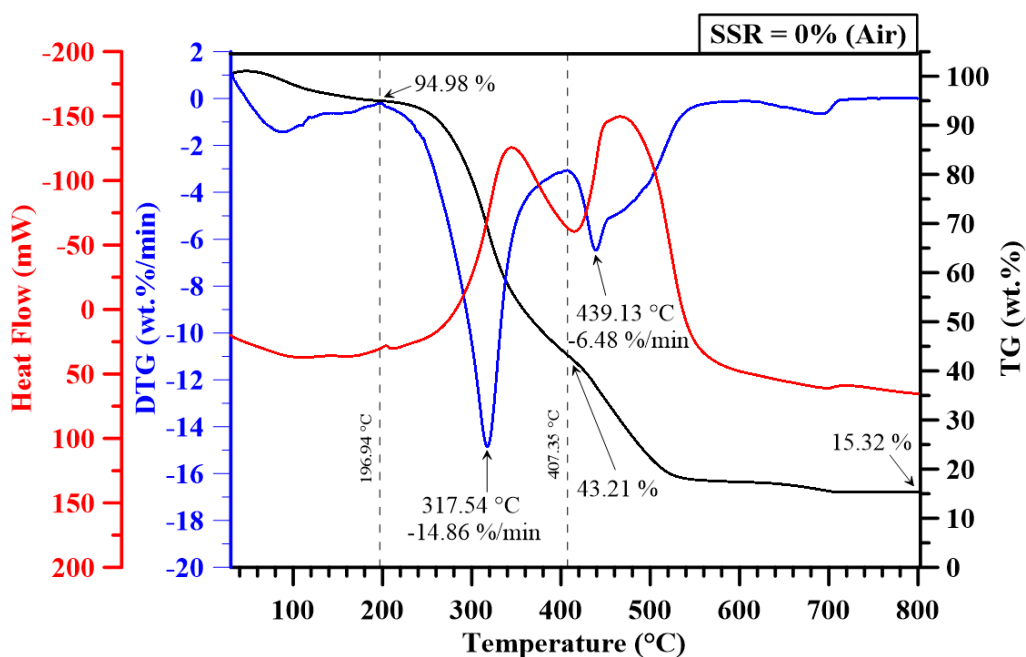

Figure 5. Thermogravimetric analysis results of shiitake substrate under combustion condition.

3.3. Synergistic Effect Analysis

The prediction of the TG curves in Figures 6 and 7 for the blends using Equations (1) and (2) revealed that they are non-additive and therefore might show some synergistic effects. A comparison of the weight loss from the experimental TGA curves for various BBRs to that calculated from the linear additive rule is shown in Figure 8 for the sludge-coal blends. The figure shows the various trends of W_{exp} and W_{cal} for the different blends for $\beta = 20\ °C·min^{-1}$. For the BBR = 25% blend, the residual

values of the experimental curve were lower than those of the calculated curve between 600 and 800 °C. This suggests that a positive synergistic effect may exist between coal and sludge for this blend in this temperature range. A similar tendency can be seen in Figure 9 for all sludge-shiitake blends at higher temperatures. In contrast, the residual values of the experimental curve for BBR = 50% and 75% were greater than the calculated values, implying negative synergy.
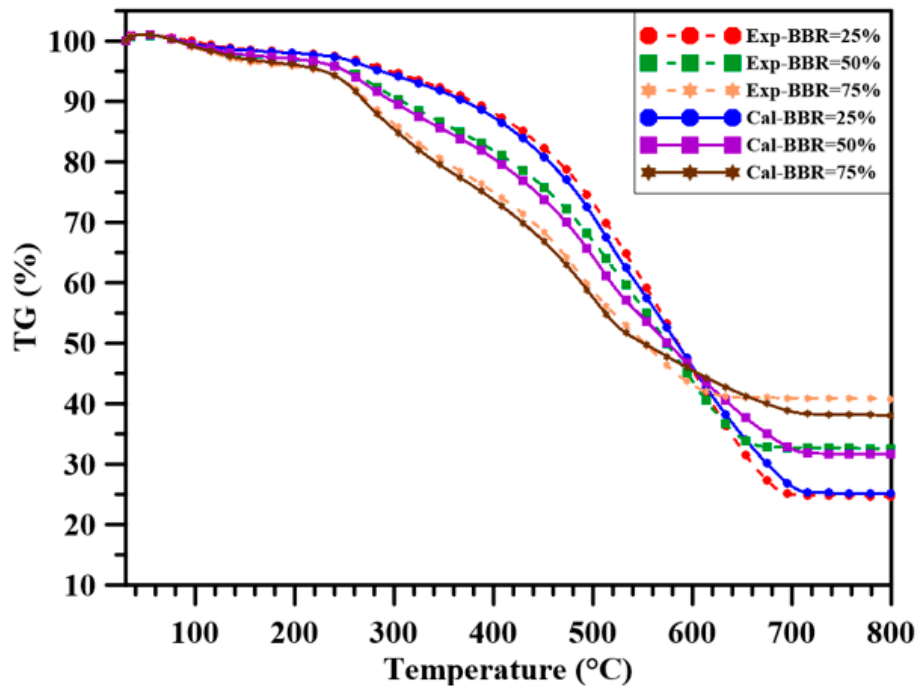

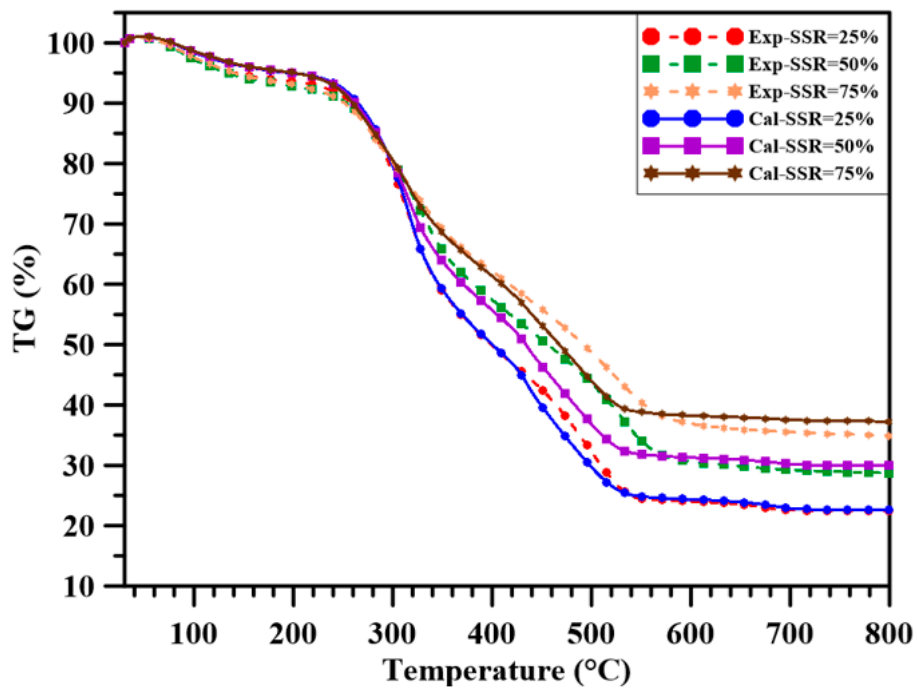**Figure 6.** Synergistic effect for various sludge-coal ratios.

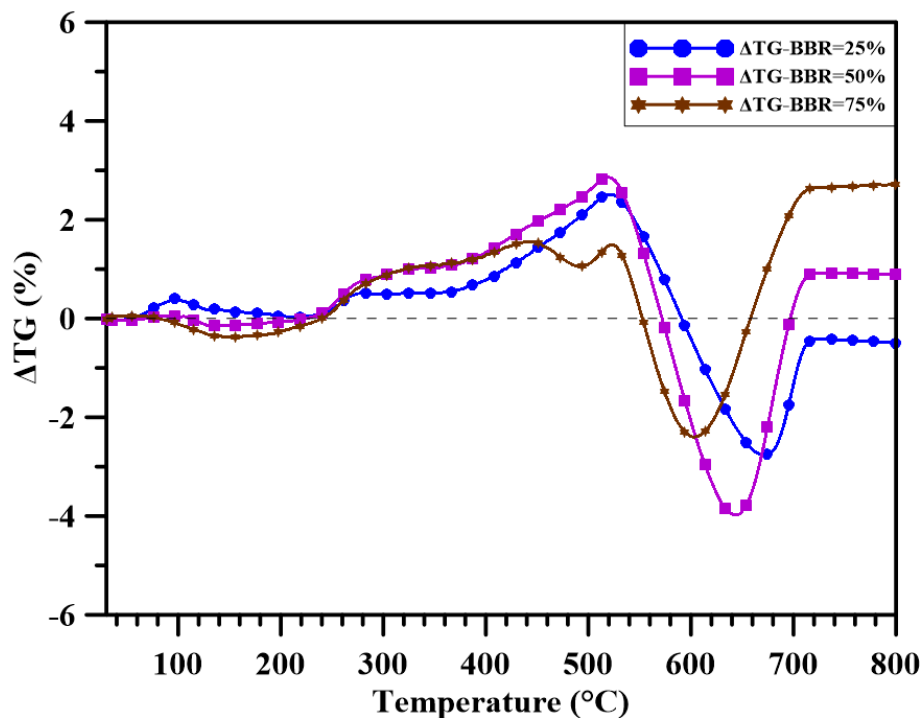**Figure 7.** Synergistic effect for various sludge-shiitake ratios.

Figure 8. Degree of synergistic effect for various sludge-coal ratios.
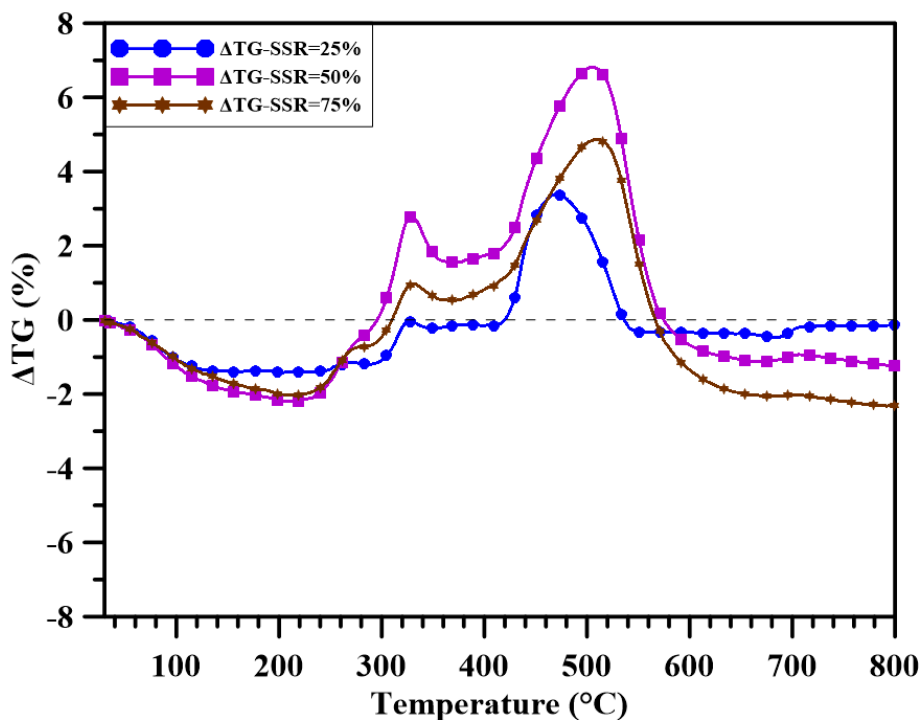

Figure 9. Degree of synergistic effect for various sludge-shiitake ratios.

Plots of the deviation between the experimental and calculated curves are shown in Figures 8 and 9. Those two figures clearly show that synergistic effects exist in the blends to a certain extent. For the BBR blends, positive synergy occurred during char oxidation. The catalytic effects of the sludge char might promote reactions at high temperature. However, at low temperature, the large quantity of released volatiles from the sludge may hinder the release of volatiles from the coal, which explains the negative synergistic effect. For the SSR blends, the addition of shiitake to the blends promoted reactions in the blend at both high and low temperatures. For all the blends, negative or low synergistic

effects existed for temperatures between 300 and 500 °C. The values of the root mean square (RMS) of ΔW were all between 1.06 and 1.57 for the blends, higher than those used to measure synergistic effects and reported in previous studies [23,30], indicating that there were synergistic effects in the blends.

3.4. Combustion Characteristics Parameters

The combustion characteristics for the sludge-coal blends are shown in Table 3. Sludge high porosity and high surface area can explain why its devolatilization started at a lower temperature compared to the other fuels, and this led to a decrease in the ignition temperature with sludge addition to the blends in stage 1. Increasing sludge content in the blends resulted in an increase in burnout temperature in stage 1. Sewage sludge having higher devolatilization rate than Australian coal can explain why both the maximum and mean burning rates increased for the blends in the main oxidation stage (stage 1) with increasing sludge ratio, which also explained the increase in the values calculated for both the flammability index and the combustion characteristics index. The highest values for C and S in stage 1 for the blend were observed for BBR = 75% ($C_1 = 5.72 \times 10^{-5}$ and $S_1 = 3.91 \times 10^{-7}$, respectively). Sludge, having less material in the final decomposition stage (stage 2), showed the lowest maximum and mean burning rate values, and thus had the lowest values for both indexes. Positive synergistic effects in the blends decreased their burnout temperature. Although T_{b2} decreased with sludge addition to the blends, the flammability index and combustion characteristics index values decreased due to the decrease of the maximum and mean burning rates. The lowest values for both indexes in stage 2 were observed for BBR = 75%, and they are $C_2 = 2.15 \times 10^{-5}$ and $S_2 = 1.01 \times 10^{-7}$, respectively. On the other hand, sludge addition to the blends resulted in an increase in the ignition temperature, up to BBR = 50%, which then decreased with further sludge addition in stage 2.

The combustion characteristics for the sludge-shiitake blends are also shown in Table 3. As shown, the ignition and burnout temperatures of the blends both increased with shiitake addition in stage 1. The results also show that the flammability index and combustion characteristics index of the shiitake substrate have the highest values among SSRs for the main oxidation stage, namely, $C_1 = 19.30 \times 10^{-5}$ and $S_1 = 33.56 \times 10^{-7}$, respectively. The Shiitake high devolatilization rate may explain why both the maximum and mean burning rates of the blends in the main decomposition stage were higher for the blends with lower sludge ratio. As a result, both the flammability index and the combustion characteristics index in stage 1 decreased with increasing sludge ratio in the blends. C and S values increased from $C_1 = 9.12 \times 10^{-5}$ and $S_1 = 10.39 \times 10^{-7}$ for SSR = 25% to $C_1 = 14.61 \times 10^{-5}$ and $S_1 = 19.42 \times 10^{-7}$ for SSR = 75%. In the final oxidation stage (stage 2), the flammability index and the combustion characteristics index values of shitake are $C_2 = 3.56 \times 10^{-5}$ and $S_2 = 0.96 \times 10^{-7}$, respectively. A 25 wt.% addition of shiitake to the blend (SSR = 75%) increased both indexes of pure sludge, resulting from increases in the values of the maximum and mean burning rates of the blend. The values of C and S both decreased for SSR = 50%, with further shiitake addition, due to the synergistic effects between shiitake and sludge at higher temperatures. The highest value for the flammability index of the blends, $C_2 = 2.29 \times 10^{-5}$, was found for SSR = 25%. The highest values for the combustion characteristics index, $S_2 = 0.66 \times 10^{-7}$, was found for SSR = 75%.

Table 3. Combustion characteristics for different sludge-coal ratios (BBR) and sludge-shiitake ratios (SSR) (BBR = SSR = 100%: pure sludge).

BBR %	T_i		T_b		DTG_{max}		DTG_{mean}		$C \times 10^5$		$S \times 10^7$	
	T_{i1}	T_{i2}	T_{b1}	T_{b2}	Stage 1	Stage 2	Stage 1	Stage 2	C_1	C_2	S_1	S_2
0	-	438.29	-	709.15	-	6.33	-	5.15	-	3.30	-	2.39
25	247.30	458.42	306.90	693.62	1.13	5.68	0.96	4.68	1.85	2.70	0.58	1.82
50	240.97	462.41	357.28	665.57	2.11	4.74	1.77	3.93	3.64	2.22	1.81	1.31
75	238.31	446.67	367.44	629.45	3.25	4.29	2.51	2.95	5.72	2.15	3.91	1.01
100	239.40	439.32	368.57	633.29	4.80	3.94	3.48	1.65	8.37	2.04	7.90	0.53
SSR %	T_i		T_b		DTG_{max}		DTG_{mean}		$C \times 10^5$		$S \times 10^7$	
	T_{i1}	T_{i2}	T_{b1}	T_{b2}	Stage 1	Stage 2	Stage 1	Stage 2	C_1	C_2	S_1	S_2
0	277.43	426.59	404	680.82	14.86	6.48	7.02	1.83	19.30	3.56	33.56	0.96
25	272.38	457.96	417.81	666.85	10.84	4.80	5.56	1.68	14.61	2.29	19.42	0.58
50	266.82	469.67	413.85	688.17	6.95	3.52	4.49	1.67	9.76	1.59	10.59	0.39
75	253.93	436.20	379.99	620.62	5.88	4.14	4.33	1.89	9.12	2.18	10.39	0.66
100	239.40	439.32	368.57	633.29	4.80	3.94	3.48	1.65	8.37	2.04	7.90	0.53

3.5. Kinetic Parameters Analysis

According to the fitting results of linear regression using various kinetic mechanism equations, reaction orders of 1.2 and 1.5 were found to be the best model functions for stage 1 and stage 2, respectively; with corresponding correlation coefficients ranging from 0.950 to 0.994. The results of the calculated activation energy and frequency factor are shown in Table 4. As shown, the calculated E and A for stage 1 of sewage sludge are 80.42 kJ·mol^{-1} and 6.18×10^{12} s^{-1}, respectively. Those for shiitake are 97.07 kJ·mol^{-1} and 1.46×10^{14} s^{-1}, respectively. This shows that more energy is needed for the combustion of the volatiles in the shiitake substrate during stage 1. The kinetic parameters of the blends are non-additive, and therefore their values could not be predicted. BBR = 25% could be divided into two oxidation stages, and the calculated activation energy and frequency factor for stage 1 are 85.68 kJ·mol^{-1} and 2.80×10^{12}·s^{-1}, respectively. The addition of 50 wt.% sludge resulted in a decrease of both parameters due to the catalytic effect of sludge addition to the blend. Further sludge addition to the blend resulted in increases in both the activation energy and the frequency factor. This might be due to the occurrence of secondary reactions in the main oxidation stage. The activation energy and the pre-exponential factor are $E_1 = 80.90$ kJ·mol^{-1} and $A_1 = 3.83 \times 10^{12}$ s^{-1}, respectively, for BBR = 75%. For the sludge-shiitake blends, increases in both the activation energy and the frequency factor were observed in stage 1 with shiitake addition to the blends, except when 50 wt.% shiitake was added to the sludge, as shown in Table 4.

Table 4. Kinetic parameters for various sludge-coal ratios and sludge-shiitake ratios calculated using Coats-Redfern method (BBR = SSR = 100%: pure sludge).

BBR %	Temperature Range (°C)	E (kJ·mol^{-1})	A (s^{-1})	N	R^2
	-	-	-	-	-
0	278–730	105.74	1.06×10^{13}	1.20	0.971
25	210–308	85.68	2.80×10^{12}	1.50	0.991
	309–714	59.27	4.93×10^{9}	1.20	0.994
50	203–359	75.18	4.83×10^{11}	1.50	0.969
	360–692	54.70	3.48×10^{9}	1.20	0.993
75	202–369	80.90	3.83×10^{12}	1.50	0.950
	370–673	70.89	1.66×10^{11}	1.20	0.964
100	200–370	80.42	6.18×10^{12}	1.50	0.960
	371–624	64.89	1.07×10^{11}	1.20	0.981
SSR %	Temperature Range (°C)	E (kJ·mol^{-1})	A (s^{-1})	N	R^2
0	206–408	97.07	1.46×10^{14}	1.50	0.972
	408–579	62.93	8.23×10^{10}	1.20	0.989
25	206–432	87.00	1.55×10^{13}	1.50	0.956
	432–562	75.30	5.97×10^{11}	1.20	0.980
50	200–417	79.25	2.98×10^{12}	1.50	0.977
	417–632	61.80	4.38×10^{10}	1.20	0.983
75	194–382	84.33	1.25×10^{13}	1.50	0.982
	383–648	61.83	6.05×10^{10}	1.20	0.994
100	200–370	80.42	6.18×10^{12}	1.50	0.960
	371–624	64.89	1.07×10^{11}	1.20	0.981

A comparison of the activation energy values of the individual fuels in the final oxidation stage shows that Australian black coal has the highest value for E (105.74 kJ·mol^{-1}), as expected. The values for sludge and shiitake are 64.89 and 62.93 kJ·mol^{-1}, respectively. The catalytic effect of sludge addition to the blends was also noticed in the final oxidation stage. The activation energy and the pre-exponential factor both decreased with sludge addition, except for BBR = 75%, due to the occurrence of secondary reactions. The inorganic materials in the sludge catalytically promoted char formation and tar-cracking reactions in the sludge-coal blends, and the lignin in the substrate produced the same effect to the sludge-shiitake blends, which is shown by a decrease in the calculated E values for the sludge-shiitake blends. A previous study found that the presence of alkaline salts in biomass may lower the apparent activation energy of thermal reactions and promote the formation of

char [36]. However, the opposite effect was observed with further addition of sludge and shiitake to the sludge-coal and sludge-shitake blends, respectively, due to further reactions between the heavier and complex compounds in the fuels.

3.6. Fourier Transform Infrared Spectroscopy

Figure 10 shows the CH_4 emission profiles for the sludge, the Australian black coal and their blends. The curve for sewage sludge shows two peaks, one at 280 °C and the other one at 474 °C, corresponding to two burning regions involving volatiles and fixed carbon. The release of CH_4 during the final decomposition stage was much lower than that in the main decomposition stage. The release of CH_4 in stage 1 is due to the primary pyrolysis of the volatiles and the cellulose in the sludge. A significant amount of the cellulose is converted into tar during the primary pyrolysis, and then some residual parts of the tar are converted into gases during the secondary reaction, which explains the occurrence of the second peak. The Australian coal, having low amount of volatile and one thermal decomposition stage, has one main peak around 471 °C. Adding sludge to the blends increased the amount of CH_4 released in the main decomposition stage, but decreased that of stage 2. The peaks for 25 wt.% sludge appeared to be the lowest. This was confirmed by taking the integral area under the curves and evaluating the gas yield using Equation (13). The results are shown in Table 5. They reveal that BBR = 25% yielded the lowest amount of CH_4. Figure 10 also shows the CH_4 emission profiles for the sludge-shiitake blends. Shiitake, having higher volatile and fixed carbon content than that of sludge, released a higher amount of CH_4 in both the main and final decomposition stages compared to that released by sludge. Adding shiitake to the blends reduced both peaks to approximately the same absorbance range, with SSR = 50% having the lowest peak for both stages. As shown in Table 5, adding sludge to the blends increased the amount of CH_4 emitted, and SSR = 25% showed the lowest methane emission.

The CO emission profiles for the individual fuels and their blends are shown in Figure 11. Only one absorption peak was observed for coal and the sludge-coal blends. In contrast, all profiles of the sludge-shiitake blends showed two peaks, in the temperature ranges of 275–400 °C and 425–575 °C, respectively. The first CO peak for sludge was observed at about 341 °C and the second one was observed at about 495 °C. The CO generation of stage 1 and stage 2 was attributed to the decomposition of the volatiles and decarbonylation reaction, respectively. Adding sludge to the blends reduced the absorption value of their peak, which is consistent with the results in Table 5. BBR = 75% yielded the lowest value (0.078). However, adding shiitake to the sludge-shiitake blends increased the CO emission in stage 1, which was compensated with a reduction in CO in stage 2. Overall, CO emission of the blends decreased with shiitake addition to the blends, with SSR = 25% having the lowest gas yield value (0.049).
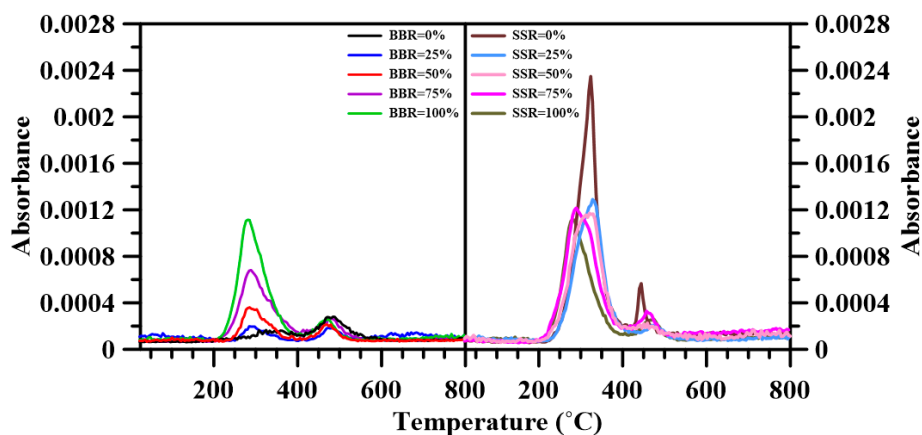

Figure 10. Evolution of CH_4 for various sludge-coal and sludge-shiitake ratios in TGA-FTIR.

Table 5. Evolved gas production rates of different sludge-coal ratios (BBR) and sludge-shiitake ratios (SSR) (BBR = SSR = 100%: pure sludge).

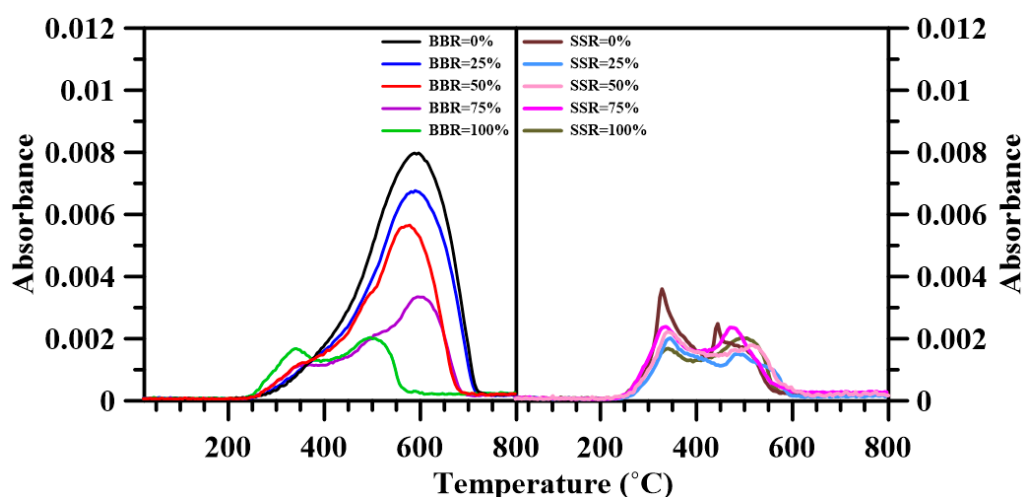| BBR %	CH_4	CO	CO_2	NO_x	SO_2
0%	0.010	0.186	5.035	0.275	0.180
25%	0.009	0.146	4.114	0.228	0.150
50%	0.010	0.124	3.757	0.271	0.180
75%	0.013	0.078	2.324	0.268	0.180
100%	0.017	0.052	2.042	0.337	0.227
SSR %	CH_4	CO	CO_2	NO_x	SO_2
0%	0.023	0.060	3.492	0.259	0.166
25%	0.018	0.049	2.466	0.203	0.131
50%	0.019	0.055	2.598	0.240	0.152
75%	0.021	0.061	2.639	0.296	0.195
100%	0.017	0.052	2.042	0.337	0.227

Figure 11. Evolution of CO for various sludge-coal and sludge-shiitake ratios in TGA-FTIR.

Figure 12 shows the CO_2 emission profiles of the respective fuels and their blends. All profiles displayed only one peak. The peak of the sludge-coal blends occurred at higher temperature, 425–700 °C, compared to that of the sludge-shiitake blends, which was observed between 300–600 °C. As shown in Figure 12, sludge addition to the blends decreased the amount of CO_2 emitted. BBR = 75% showed the lowest value of the yielded CO_2 of the blends, as shown in Table 5. In contrast, an addition of 25 wt.% shiitake to sludge led to an increase of about 30% for CO_2 emissions, as shown in Table 5. However, CO_2 emission decreased with further shiitake addition to the blends.

NO_x formation during fuel combustion arises from three possible routes, thermal-NO_x, prompt-NO_x and fuel-NO_x [35]. Generally, thermal-NOx is generated from thermal oxidation of nitrogen at high temperature (>1500 °C). Although its emission increases with increasing oxygen concentration and combustion temperature, its role is negligible at temperatures below 1500 °C, as is the case in this study. The formation of prompt-NO_x is more complex, involving CH radical intermediates that react with the nitrogen in air to form HCN, which further reacts to generate NO. The fuel-NO_x formation mechanism is even more complicated. It is formed from the nitrogen content in the fuel via two routes: (1) by homogeneous reactions of the nitrogenous compounds of the volatiles and (2) via heterogeneous reactions of the nitrogen components bound to the char. For the experiments conditions in this study, most of the NO_x came from fuel-NO_x. Figure 13 shows the NO_x emission profiles of the individual fuels and their blends, showing one peak between 250 °C and 375 °C, which indicates significant NO emission produced by the volatile-N oxidation, for all the blends.

Sewage sludge, having the highest nitrogen content yielded the highest NO_x of the fuels. The yielded values of NO_x emission in Table 5 are all lower than that of pure coal, with NO_x emissions of BBR = 25% being the lowest. A similar observation was made for the yielded NO_x values for the sludge-shiitake blends in Table 5, with a decrease in NO_x emissions found with increasing shiitake ratio. The oxides in the char/ash play an active role in NO_x reduction. Lower oxygen concentration in the oxidizer was beneficial for reducing NO_x. As the volatiles in the blends increased, their combustion consumed the oxygen near the char particles, and therefore decreased the oxygen concentration around the char.
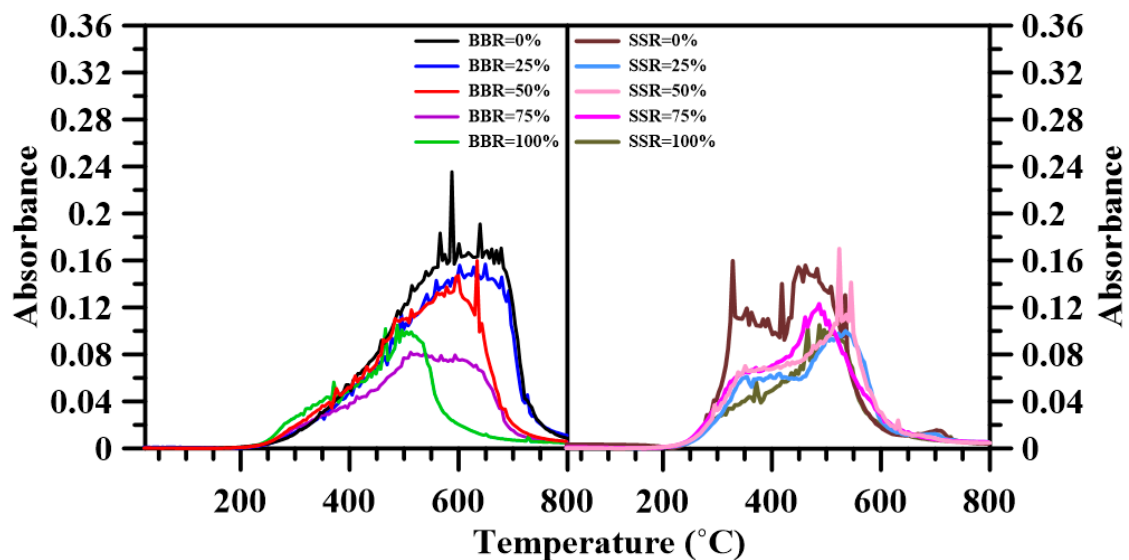

Figure 12. Evolution of CO_2 for various sludge-coal and sludge-shiitake ratios in TGA-FTIR.
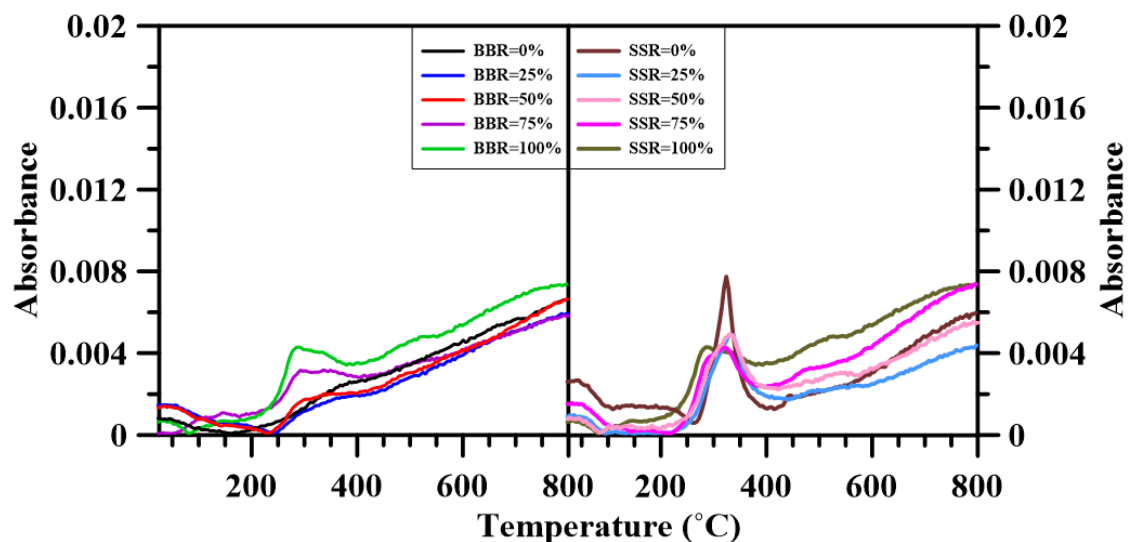

Figure 13. Evolution of NO_x for various sludge-coal and sludge-shiitake ratios in TGA-FTIR.

Figure 14 shows the SO_2 emission profiles for the individual fuels and their blends. As shown, all curves have smooth peaks, except the shiitake one. SO_2 generation was closely related to the sulfur content in the fuels, as shown by the results of Table 5. Sewage sludge, having the highest sludge content, showed the highest values of yielded SO_2. An addition of 25 wt.% sludge to the sludge-coal blends reduced the amount of yielded SO_2. An increase of SO_2 emission was observed with sludge further addition. The alkali and alkaline earth metal oxides in the sludge might act as a desulfurizing catalyst for such blends. However, further sludge addition of sludge increased

the amount of yielded SO_2. For the sludge-shiitake blends, increasing the shiitake ratio decreased SO_2 emissions.
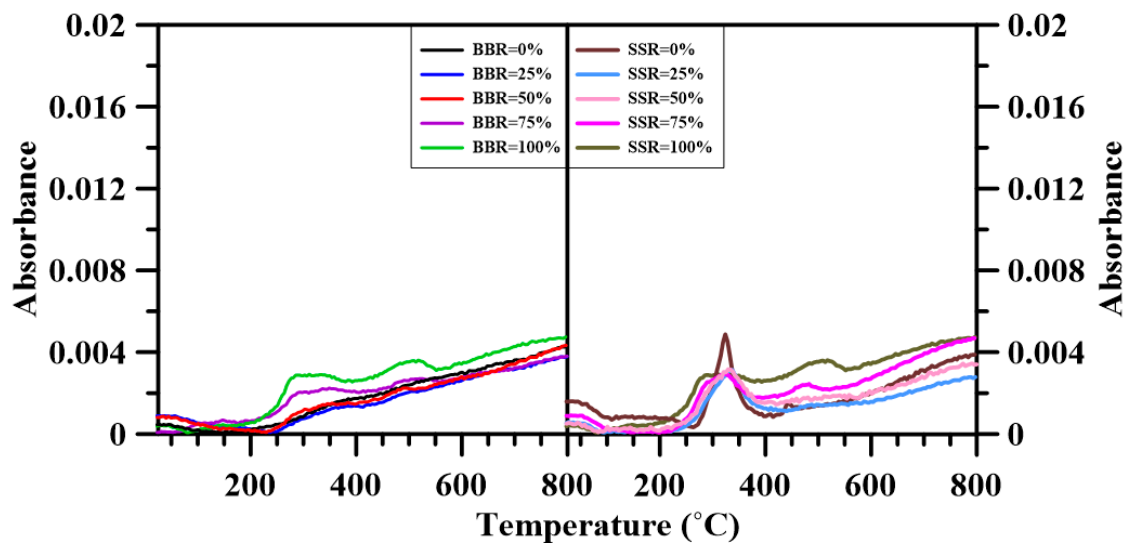

Figure 14. Evolution of SO_2 for various sludge-coal and sludge-shiitake ratios in TGA-FTIR.

In summary, BBR = 25% showed the lowest CH_4, NO_x and SO_2 emissions. The values of emitted CO and CO_2 decreased with addition of sludge to the blends. NO_x and SO_2 emissions both decreased with shiitake addition to the sludge-shiitake blends. An addition of 25 wt.% shiitake to the sludge increased the amount of CH_4, CO and CO_2. However, further shiitake addition decreased their respective yields.

3.7. Single-Pellet Combustion

The combustion process of a pure sludge pellet and the way used to demarcate some of the parameters are shown in Figure 15 for ambient temperatures of 700 °C. They show the volatiles, from the pellet, burning in the gas phase after the pellet fell into the hot environment before extinguishing. Then, char oxidation occurs homogeneously until burnout. The results of the studied parameters for the blends, i.e., ignition delay time (t_{id}), volatile combustion duration (t_f), and total combustion time (t_{tot}) for the single-pellet combustion experiments at 600 °C, 700 °C and 800 °C are shown in Tables 6 and 7. The weight loss history and its first derivative for pure sewage sludge pellet at 700 °C are presented in Figure 16 for illustration. Different temperatures have similar trends. An abrupt change in the pellet weight could be noticed during the devolatilization and volatiles combustion stage, whereas char combustion occurred at an almost constant weight loss rate until burnout.
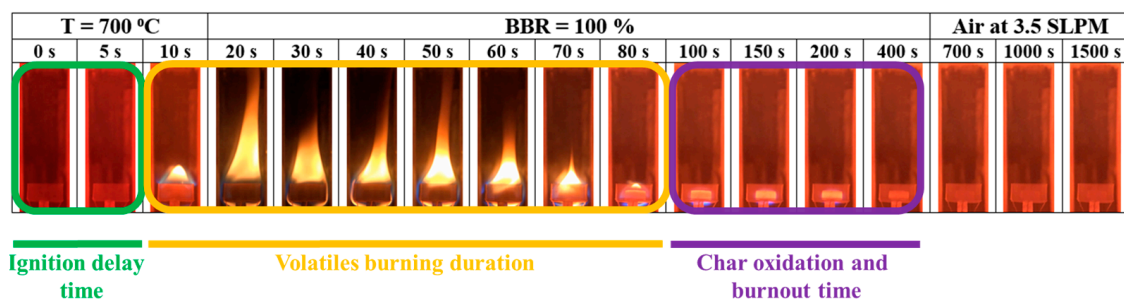

Figure 15. Graphic of stages in pure sewage sludge pellet combustion process.

Table 6. Single-pellet combustion characterization for various sludge-coal ratios (BBR = SSR = 100%: pure sludge).

BBR %	Single Pellet Combustion Characterization at 600 °C				HHV (MJ·kg^{-1})
	t_{id} (s)	t_f (s)	t_{tot} (s)	Ash (wt.%)	
0	Indistinct	Indistinct	1611 ± 44.69	19.63 ± 0.87	26.10 ± 0.05
25	Indistinct	Indistinct	1371.80 ± 38.71	24.01 ± 0.79	22.48 ± 0.06
50	Indistinct	Indistinct	1174.20 ± 41.67	30.53 ± 0.19	18.64 ± 0.18
75	Indistinct	Indistinct	904.50 ± 27.93	36.46 ± 0.32	15.17 ± 0.03
100	26.27 ± 4.82	73.92 ± 2.07	615.6 ± 39.60	41.86 ± 0.82	11.91 ± 0.05
BBR %	Single Pellet Combustion Characterization at 700 °C				HHV (MJ·kg^{-1})
	t_{id} (s)	t_f (s)	t_{tot} (s)	Ash (wt.%)	
0	9.04 ± 0.66	75.94 ± 1.83	1634.80 ± 41.89	18.23 ± 1.22	26.10 ± 0.05
25	7.22 ± 0.49	83.89 ± 2.38	1517.40 ± 100.34	23.94 ± 0.23	22.48 ± 0.06
50	6.71 ± 0.28	82.23 ± 0.10	1179.80 ± 82.01	30.19 ± 0.58	18.64 ± 0.18
75	7.14 ± 0.42	80.62 ± 2.06	894 ± 22.77	34.96 ± 0.94	15.17 ± 0.03
100	7.60 ± 0.39	69.03 ± 0.48	519.40 ± 19.70	41.76 ± 1.14	11.91 ± 0.05
BBR %	Single Pellet Combustion Characterization at 800 °C				HHV (MJ·kg^{-1})
	t_{id} (s)	t_f (s)	t_{tot} (s)	Ash (wt.%)	
0	3.67 ± 0.32	73.30 ± 1.20	1534.60 ± 29.12	17.58 ± 0.51	26.10 ± 0.05
25	2.75 ± 0.21	76.88 ± 1.59	1223.40 ± 36.59	23.28 ± 0.46	22.48 ± 0.06
50	2.47 ± 0.18	75.88 ± 0.96	1031.80 ± 27.68	29.12 ± 1.08	18.64 ± 0.18
75	3.04 ± 0.19	68.47 ± 0.54	783.60 ± 41.21	34.39 ± 0.44	15.17 ± 0.03
100	3.47 ± 0.07	61.49 ± 2.09	458 ± 21.62	40.90 ± 1.15	11.91 ± 0.05

Table 7. Single-pellet combustion characterization for various sludge-shiitake ratios.

| SSR %	Single Pellet Combustion Characterization at 600 °C				HHV (MJ·kg^{-1})
	t_{id} (s)	t_f (s)	t_{tot} (s)	Ash (wt.%)	
0	19.52 ± 3.61	86.89 ± 3.01	689.6 ± 12.92	13.43 ± 1.06	16.65 ± 0.06
25	27.10 ± 0.96	77.64 ± 0.65	646.40 ± 19.74	22.95 ± 0.49	15.20 ± 0.01
50	34.94 ± 0.51	68.53 ± 1.00	618.40 ± 22.42	29.82 ± 0.63	14.03 ± 0.06
75	33.47 ± 6.22	67.12 ± 5.53	597.40 ± 29.21	37.40 ± 0.28	12.69 ± 0.02
100	26.27 ± 4.82	73.92 ± 2.07	615.6 ± 39.60	41.86 ± 0.82	11.91 ± 0.05
SSR %	Single Pellet Combustion Characterization at 700 °C				HHV (MJ·kg^{-1})
	t_{id} (s)	t_f (s)	t_{id} (s)	Ash (wt.%)	
0	5.36 ± 0.59	84.91 ± 1.65	602.20 ± 21.01	13.70 ± 0.61	16.65 ± 0.06
25	5.48 ± 0.44	79.88 ± 2.43	599.40 ± 33.28	22 ± 0.43	15.20 ± 0.01
50	6.69 ± 0.54	78.76 ± 1.06	578.20 ± 30.72	28.53 ± 1.08	14.03 ± 0.06
75	7.54 ± 0.51	73.72 ± 1.06	572.80 ± 13.14	36.42 ± 1.10	12.69 ± 0.02
100	7.60 ± 0.39	69.03 ± 0.48	519.40 ± 19.70	41.76 ± 1.14	11.91 ± 0.05
SSR %	Single Pellet Combustion Characterization at 800 °C				HHV (MJ·kg^{-1}) t_f (s)
	t_{id} (s)	t_f (s)	t_{tot} (s)	t_{id} (s)	
0	2.16 ± 0.18	77.53 ± 1.20	0	2.16 ± 0.18	77.53 ± 1.20
25	2.27 ± 0.50	76.60 ± 1.21	25	2.27 ± 0.50	76.60 ± 1.21
50	3.00 ± 0.04	72.41 ± 0.07	50	3.00 ± 0.04	72.41 ± 0.07
75	3.03 ± 0.34	67.17 ± 1.25	75	3.03 ± 0.34	67.17 ± 1.25
100	3.47 ± 0.07	61.49 ± 2.03	100	3.47 ± 0.07	61.49 ± 2.03
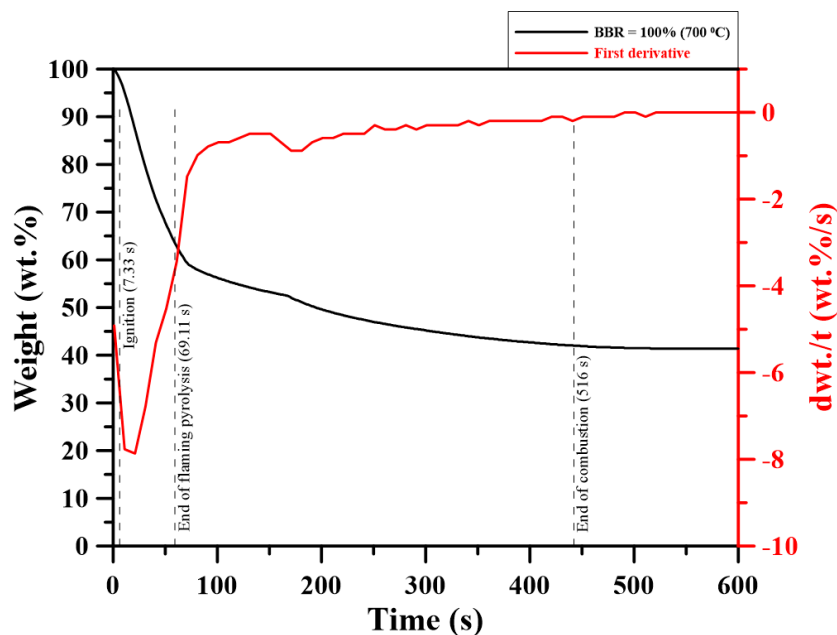
Figure 16. Weight loss history of pure sewage sludge pellet combustion process at 700 °C.

At 600 °C, the pure sludge pellets (BBR = 100%) took on average 26.27 s to ignite. No gas-phase ignition occurred for pure coal pellets and sludge-coal blends pellets with BBR = 25–75%. This might be because the volatiles released from Australian coal and the blends have an auto-ignition temperature that is higher than 600 °C. As shown from the FTIR experiments, the hydrocarbons released from the devolatilization process of the blends with BBR= 25–75% (peaks at 225–425 and 425–550 °C) turned into CO at higher temperature (peak between 550–650 °C), which then oxidized. Methane and carbon monoxide auto-ignition temperature was reported to be higher than 600 °C [37,38]. However, in contrast to the sludge-coal pellets, all the sludge-shiitake pellets ignited at 600 °C. This is consistent with the FTIR results, which shows that the hydrocarbons released from the devolatilization process of the blends with SSR= 25–75% (peaks at 200–400 and 400–500 °C) turned into CO at lower temperature (peaks between 250–475 and 475–575 °C) than those in sludge-coal blends, which then oxidized.

All the BBR pellets ignited in the gas phase at 700 °C. It took on average 7.60 s for the pellets made of sewage sludge to ignite, and pure coal pellets ignited after 9.04 s. Sludge pellets, having more volatiles content, took less time to ignite compared to pure coal ones; as predicted by Equation (15). The ignition delay time decreased for BBR = 25% and 50%. The addition of sludge to the blends increased their volatiles content, resulting in a decrease of their ignition delay time. The slight increase in ignition delay time, might be due to the endothermic evaporation of moisture delayed volatiles evolution. Adding more sludge to the blend might increase the required drying time. A similar trend was observed at 800 °C. Higher volatile content of shiitake explains why pellets made of pure shiitake took the lowest amount of time to ignite, as shown in Table 7. Adding shiitake to the blends decreased their ignition delay time.

The combustion of volatiles, t_f, is an important step in the combustion process of solid fuels, as the maximum weight loss takes place in this stage. Although the sludge volatile content is higher than that of coal, the pure coal pellet flame lasted longer than that of pure sludge pellets. A majority of the volatiles in the sludge pellet vaporized before homogeneous gas phase combustion took place. Adding 25 wt.% sludge to the blend increased the volatile combustion duration from 75.94 to 83.89 s at 700 °C, which is due to the increased volatiles content of the blend. A decrease in the volatile combustion duration was observed for blends with sludge content greater than or equal to 50 wt.%. Pellets with a higher sludge ratio have more volatiles and, in theory, should have a longer volatile combustion duration. However, conducting TGA experiments of sewage sludge under pyrolysis conditions shows that volatiles in sludge escape at a higher rate in sludge than in coal. Therefore,

the volatile combustion duration reduced for BBR = 50–75% pellets. Moreover, the pure sludge pellet volatile flame lasted 69.03 s on average, the shortest time. On average, volatile combustion took about 13.36% of the total combustion time for the pure sludge pellets; for pure coal pellet, volatile combustion took about 4.71% of the total combustion time at 700 and 800 °C. Single-pellet combustion experiments conducted at 800 °C showed similar patterns to those observed at 700 °C. For the sludge-shiitake blends, t_f increased with shiitake addition to the blends. On average, volatile combustion took about 14.10% of the total combustion time for the pure shiitake pellets, 13.29% for the pure sludge pellets, and 4.65% for the pure coal pellets.

The total combustion (t_{tot}) time for various BBR pellets is also shown in Table 6. As expected, the total combustion time of the coal pellet was much greater than that of the sludge pellet. Since coal has more fixed carbon content than does sewage sludge, its char oxidation takes longer than that of sludge at the same ambient temperature, which explains why pure coal pellets had the longest total combustion time. A linear decrease in the total combustion time was observed with the addition of sludge to the blends, with the pure sludge pellets having the shortest total combustion time. Char formed from sludge is more reactive than that of coal and possesses more pores and thus takes less time to burnout. This explains why the addition of sewage sludge to the blends significantly decreased their total combustion time for all ambient temperatures. As shown in Table 7, the char of the shiitake pellets, having more fixed carbon, took more time to burnout than that of the sludge pellet. A linear increase in the total combustion time was observed with shiitake addition to the blend, due to the increase in fixed carbon content in the blends. Shiitake addition to the sludge can help with the issues related to ash, such as de-ashing, ash transport, storage, and disposal. Shiitake addition to the sludge may also minimize fouling, as the blend deposited ash might retain the low-melting-point salts in sludge.

Sewage sludge, having higher inorganic content than coal, left on average more residues after the pellet combustion experiments. About 41.50% of the initial weight of the sludge pellet was left on the stainless mesh platform. The pure coal pellets left, on average, a residual weight of about 18.48%. As shown in Table 6, ash formed in the single-pellet combustion experiments increased with the addition of sewage sludge to the blends. Experiments conducted at higher temperatures showed that a high temperature in the combustor enhanced the volatilization of some of the ash-forming heavy metals resulting in lower residues. However, it should be mentioned that such a decrease in bottom ash might cause an increase in the amount of fly ash carried with the flue gas. Shiitake addition to the sludge can help with the issues related to ash, such as de-ashing, ash transport, storage, and disposal. Shiitake addition to the sludge may also minimize fouling, as the blend deposited ash might retain the low-melting-point salts in sludge. The results in Table 7 show that shiitake addition to the blends decreased the amount of ash formed in the single-pellet combustion experiments.

The heating values of the blended fuels were measured, and the results are shown in the last column in Tables 6 and 7 for reference. As shown, adding sludge to the blends decreased their HHV, with the HHV for BBR = 25% and 75% being 22.48 and 15.17 MJ·kg^{-1}, respectively. Adding shiitake to the sludge also had a positive effect on the heating values of the blended fuels. As the heating value of the blended fuels increased with shiitake addition. The heating values for SSR = 75% and 25% being 12.69 and 15.20 MJ·kg^{-1}, respectively.

4. Conclusions

In this study, the combustion behavior of sewage sludge, Australian black coal, a shiitake substrate, and their blends was analyzed via thermogravimetric analysis and FTIR analysis. The findings can be summarized as follow:

1. Compared to both the shiitake substrate and Australian coal, dried sewage sludge has the lowest carbon content and the highest nitrogen and sulfur content. Furthermore, the sludge hydrogen and oxygen content levels are higher than those of Australian black coal, but lower than those of the shiitake substrate. Sewage sludge has the lowest HHV. However, on a dry and ash-free basis,

its HHV is similar to that of shiitake. The proximate analysis results show that sewage sludge has the lowest fixed carbon content and the highest ash content on an as-received basis of the fuels. The shiitake substrate has the highest amount of volatiles.

2. Both pure sludge and shiitake have higher flammability index and combustion characteristics index in the main decomposition stage compared to those of coal. Sludge addition to coal increased both indexes in stage 1 and a similar observation was made for the sludge-shiitake blends with shiitake addition to the sludge. In the final oxidation stage, adding sludge to the blends decreased their flammability index and combustion characteristics index, due to the low decomposition rate of the heavier and complex compounds in the sludge. For the sludge-shiitake blends, a 25 wt.% sludge addition to the sludge increases both indexes. The flammability index and the combustion characteristics index both decreased for SSR = 50%; and then increased with 75 wt.% shiitake addition to the sludge.

3. Synergistic effects occurred for both the sludge-coal blends and sludge-shiitake blends. For all the blends, negative or low synergistic effects existed in the temperature range of 300 and 500 °C. For higher temperature, during the char oxidation stage, positive synergistic effects occurred. The addition of shiitake to the blends had positive synergy for all the blending ratios. However, when the BBR $\geq$ 50 wt.%, negative synergy occurred at high temperature.

4. The results of the kinetic parameters showed that a reduction in both parameters occurred for BBR = 50% during the main oxidation stage. A similar observation was made for the sludge-shiitake blends. The catalytic effect of the sludge and the shiitake is pronounced in the final oxidation stage. A decrease in both the activation energy and the frequency factor occurred with sludge addition to the coal due to the catalytic effect of the inorganic materials in the sludge. A similar observation was made for the sludge-shiitake blends, as the lignin in the substrate catalytically promoted the reactions in the final oxidation stage. However, due to further reactions between the heavier and complex compounds in the samples, both the activation energy and the frequency factor increased with further sludge or shiitake addition to their respective blends (BBR = 75% and SSR = 25%).

5. The FTIR results show that adding sludge to the sludge-coal blends decreased both CO_2 and CO emissions. A decrease in the emitted CH_4, NO_x and SO_2 was found for BBR = 25%. However, further addition of sludge to the blends increased their respective emissions. For the sludge-shiitake blends, both yielded values of NO_x and SO_2 decreased with shiitake addition. A 25 wt.% shiitake addition to the sludge (SSR = 75%) increased the amount of emitted CH_4, CO and CO_2. However, further shiitake addition decreased their respective yields.

6. For single-pellet combustion experiments, adding sludge to coal decreased the ignition delay time of the pellet to a certain extent. However, adding sludge to shiitake increased the ignition delay time. Volatile combustion durations of the blends were longer than those of the individual fuels, with BBR = 25%. For other cases, they decreased with sludge addition to the blends. The volatile burning duration decreased with further sludge addition. Increasing the sludge ratio sharply decreased the total combustion time and increased the percentage of residual weight (ash) in the single-pellet combustion experiments.

Author Contributions: G.-B.C. and T.-H.L. contributed to the concept, results explanation and writing of the paper. S.C. performed the experiments and analyzed the data. H.-T.L. and F.-H.W. contributed to experimental method and paper review.

References

1. Environmental Protection Administration, R.O.C. *Review of Sludge Treatment Status and Response Strategies*; Environmental Protection Administration: Taipei, Taiwan, 2014.

2. Lundin, M.; Olofsson, M.; Pettersson, G.; Zetterlund, H. Environmental and economic assessment of sewage sludge handling options. *Resour. Conserv. Recycl.* **2004**, *41*, 255–278. [CrossRef]

3. Muchuweti, M.; Birkett, J.; Chinyanga, E.; Zvauya, R.; Scrimshaw, M.D.; Lester, J. Heavy metal content of vegetables irrigated with mixtures of wastewater and sewage sludge in Zimbabwe: Implications for human health. *Agric. Ecosyst. Environ.* **2006**, *112*, 41–48. [CrossRef]

4. Werther, J.; Ogada, T. Sewage sludge combustion. *Prog. Energy Combust. Sci.* **1999**, *25*, 55–116. [CrossRef]

5. European Union. Directive 2009/28/EC of the European Parliament and of the Council of 23 April 2009 on the promotion of the use of energy from renewable sources and amending and subsequently repealing Directives 2001/77/EC and 2003/30/EC. *Off. J. Eur. Union* **2009**, *5*, 2009.

6. Vassilev, S.V.; Baxter, D.; Andersen, L.K.; Vassileva, C.G.; Morgan, T.J. An overview of the organic and inorganic phase composition of biomass. *Fuel* **2012**, *94*, 1–33. [CrossRef]

7. García, G.; Arauzo, J.; Gonzalo, A.; Sánchez, J.L.; Ábrego, J. Influence of feedstock composition in fluidised bed co-gasification of mixtures of lignite, bituminous coal and sewage sludge. *Chem. Eng. J.* **2013**, *222*, 345–352. [CrossRef]

8. Vamvuka, D.; Sfakiotakis, S.; Saxioni, S. Evaluation of urban wastes as promising co-fuels for energy production—A TG/MS study. *Fuel* **2015**, *147*, 170–183. [CrossRef]

9. Cui, H.; Ninomiya, Y.; Masui, M.; Mizukoshi, H.; Sakano, T.; Kanaoka, C. Fundamental Behaviors in Combustion of Raw Sewage Sludge. *Energy Fuels* **2006**, *20*, 77–83. [CrossRef]

10. Miller, R.; Bellan, J. Analysis of reaction products and conversion time in the pyrolysis of cellulose and wood particles. *Combust. Sci. Technol.* **1996**, *119*, 331–373. [CrossRef]

11. Koppejan, J.; van Loo, S. *The Handbook of Biomass Combustion and Co-Firing*; Earthscan: London, UK, 2008.

12. Rulkens, W. Sewage sludge as a biomass resource for the production of energy: Overview and assessment of the various options. *Energy Fuels* **2007**, *22*, 9–15. [CrossRef]

13. Stasta, P.; Boran, J.; Bebar, L.; Stehlik, P.; Oral, J. Thermal processing of sewage sludge. *Appl. Therm. Eng.* **2006**, *26*, 1420–1426. [CrossRef]

14. Roy, M.M.; Dutta, A.; Corscadden, K.; Havard, P.; Dickie, L. Review of biosolids management options and co-incineration of a biosolid-derived fuel. *Waste Manag.* **2011**, *31*, 2228–2235. [CrossRef] [PubMed]

15. Otero, M.; Díez, C.; Calvo, L.F.; García, A.I.; Morán, A. Analysis of the co-combustion of sewage sludge and coal by TG-MS. *Biomass Bioenergy* **2002**, *22*, 319–329. [CrossRef]

16. Ninomiya, Y.; Zhang, L.; Sakano, T.; Kanaoka, C.; Masui, M. Transformation of mineral and emission of particulate matters during co-combustion of coal with sewage sludge. *Fuel* **2004**, *83*, 751–764. [CrossRef]

17. Folgueras, M.B.; Díaz, R.M.; Xiberta, J.; Prieto, I. Thermogravimetric analysis of the co-combustion of coal and sewage sludge. *Fuel* **2003**, *82*, 2051–2055. [CrossRef]

18. Kijo-Kleczkowska, A.; Środa, K.; Kosowska-Golachowska, M.; Musiał, T.; Wolski, K. Experimental research of sewage sludge with coal and biomass co-combustion, in pellet form. *Waste Manag.* **2016**, *53*, 165–181. [CrossRef] [PubMed]

19. Taiwan Agricultural Research Institute Council of Agriculture, Executive Yuan, Alternative Substrates for Growing Mushrooms. Available online: https://www.tari.gov.tw/english/form/index-1.asp?Parser=20,15, 926,81,,,3007 (accessed on 22 July 2015).

20. Taiwan Business TOPICS, Fungus among Us—The History of Mushrooms in Taiwan. Available online: https://topics.amcham.com.tw/2017/01/fungus-among-us-history-mushrooms-taiwan/ (accessed on 16 January 2017).

21. Cassel, B.; Menard, K.; Shelton, C.; Earnest, C. *Proximate Analysis of Coal and Coke Using the STA 8000 Simultaneous Thermal Analyzer*; PerkinElmer Application Note; PerkinElmer: Waltham, MA, USA, 2012.

22. Wu, Z.; Wang, S.; Zhao, J.; Chen, L.; Meng, H. Synergistic effect on thermal behavior during co-pyrolysis of lignocellulosic biomass model components blend with bituminous coal. *Bioresour. Technol.* **2014**, *169*, 220–228. [CrossRef] [PubMed]

23. Sadhukhan, A.K.; Gupta, P.; Goyal, T.; Saha, R.K. Modelling of pyrolysis of coal–biomass blends using thermogravimetric analysis. *Bioresour. Technol.* **2008**, *99*, 8022–8026. [CrossRef]

24. Lu, J.J.; Chen, W.H. Investigation on the ignition and burnout temperatures of bamboo and sugarcane bagasse by thermogravimetric analysis. *Appl. Energy* **2015**, *160*, 49–57. [CrossRef]
25. Chen, G.-B.; Li, Y.-H.; Lan, C.-H.; Lin, H.-T.; Chao, Y.-C. Micro-explosion and burning characteristics of a single droplet of pyrolytic oil from castor seeds. *Appl. Therm. Eng.* **2017**, *114*, 1053–1063. [CrossRef]
26. Jin, Y.; Li, Y.; Liu, F. Combustion effects and emission characteristics of SO2, CO, NOx and heavy metals during co-combustion of coal and dewatered sludge. *Front. Environ. Sci. Eng.* **2016**, *10*, 201–210. [CrossRef]
27. Coats, A.W.; Redfern, J. Kinetic parameters from thermogravimetric data. *Nature* **1964**, *201*, 68. [CrossRef]
28. Gao, N.; Li, A.; Quan, C.; Du, L.; Duan, Y. TG–FTIR and Py–GC/MS analysis on pyrolysis and combustion of pine sawdust. *J. Anal. Appl. Pyrolysis* **2013**, *100*, 26–32. [CrossRef]
29. Xu, T.; Huang, X. Study on combustion mechanism of asphalt binder by using TG–FTIR technique. *Fuel* **2010**, *89*, 2185–2190. [CrossRef]
30. Oudghiri, F.; Allali, N.; Quiroga, J.M.; Rodríguez-Barroso, M.R. TG–FTIR analysis on pyrolysis and combustion of marine sediment. *Infrared Phys. Technol.* **2016**, *78*, 268–274. [CrossRef]
31. Fan, C.; Yan, J.; Huang, Y.; Han, X.; Jiang, X. XRD and TG-FTIR study of the effect of mineral matrix on the pyrolysis and combustion of organic matter in shale char. *Fuel* **2015**, *139*, 502–510. [CrossRef]
32. Mau, V.; Gross, A. Energy conversion and gas emissions from production and combustion of poultry-litter-derived hydrochar and biochar. *Appl. Energy* **2018**, *213*, 510–519. [CrossRef]
33. Wang, C.; Wu, Y.; Liu, Q.; Yang, H.; Wang, F. Analysis of the behaviour of pollutant gas emissions during wheat straw/coal cofiring by TG–FTIR. *Fuel Process. Technol.* **2011**, *92*, 1037–1041. [CrossRef]
34. Yao, Z.; Ma, X.; Wu, Z.; Yao, T. TGA–FTIR analysis of co-pyrolysis characteristics of hydrochar and paper sludge. *J. Anal. Appl. Pyrolysis* **2017**, *123*, 40–48. [CrossRef]
35. Law, C.K. *Combustion Physics*; Cambridge University Press: Cambridge, UK, 2006.
36. Nassar, M.M. Thermal Analysis Kinetics of Bagasse and Rice Straw. *Energy Sources* **1998**, *20*, 831–837. [CrossRef]
37. Robinson, C.; Smith, D.B. The auto-ignition temperature of methane. *J. Hazard. Mater.* **1984**, *8*, 199–203. [CrossRef]
38. Mc Dougall, I. Chapter 4—Ferroalloys Processing Equipment A2—Gasik, Michael. In *Handbook of Ferroalloys*; Butterworth-Heinemann: Oxford, UK, 2013; pp. 83–138.